Bulletin of the Mineral Research and Exploration

http://bulletin.mta.gov.tr

Assessing groundwater quality in semi-arid conditions: a geographic information systems-integrated approach using water quality index

Rihab CHOUGAR[a, b] , Fethi BAALI[a, b] , Riheb HADJI[c, d*] , Lassad GHRIEB[f] , Amor HAMAD[a, b, e] and Younes HAMED[g]

[a] Department of Earth and Univers Sciences, Faculty of Exact Sciences and Natural and Life Sciences, Echahid Larbi Tebessi University, Tebessa12002, Algeria

[b] Laboratory of Water and Environment; Faculty of Exact Sciences and Natural and Life Sciences, Echahid Larbi Tebessi University, Tebessa12002, Algeria

[c] Department of Earth Sciences, Institute of Architecture and Earth Sciences, Farhat Abbas University, Setif, Algeria

[d] Laboratory of Applied Research in Engineering Geology, Geotechnics, Water Sciences, and Environment, Farhat Abbas University, Setif, Algeria

[e] International Association of Water Resources in the Southern Mediterranean Basin, Tunisia

[f] Department of Earth and universe science, Life Sciences, Guelma University, Guelma 24000, Algeria

[g] Department of Earth Sciences, Faculty of Sciences of Gafsa, University of Gafsa, Tunisia

Research Article

ABSTRACT

Meeting freshwater demands in water-scarce regions is imperative, given challenges like hydric stress, urbanization, aridity, and population growth. This study focuses on the Tebessa aquifer system, a critical water source facing escalating demands. A primary objective is to identify actionable management strategies to improve groundwater quality dynamics in semi-arid regions. The methodology involves a comprehensive assessment of groundwater health using the Water Quality Index (WQI) approach. This method integrates diverse parameters influenced by intensive agricultural and industrial activities. Additionally, spatial relationship analysis, facilitated by Geographic Information System (GIS) technology, is employed to gain insights into complex hydrogeological processes. The multi-parameter strategy implemented results in water quality maps that highlight various ions, revealing spatial disparities and assigning quality priority classes from 'Good' to 'Poor' across the groundwater. The research, conducted in the semi-arid Tebessa-Morsott Plain, encompasses field and laboratory investigations to delineate hydrochemical traits, including alkalinity, salinity, and heightened ion concentrations. The results of the study contribute to scientific understanding by uncovering interrelationships and spatial intricacies, offering valuable insights for water resource governance. The effectiveness of the methodology, incorporating WQI and GIS, is demonstrated in the comprehensive evaluation of groundwater quality. Ultimately, this research provides a foundation for informed decision-making and sustainable management of groundwater resources in semi-arid regions.

1. Introduction

Groundwater is a critical source of potable water, especially in semiarid regions where scarce and unpredictable precipitation necessitates heavy reliance on this resource. The resilience of groundwater reserves in these areas is vital for communities facing water scarcity. However, the sustained viability of this resource hinges on its quality, and ensuring its purity is imperative for public health. Contaminants, both natural and anthropogenic, can compromise suitability for consumption, necessitating a comprehensive understanding of groundwater quality for effective management strategies.

Rigorous investigations by researchers such as Drias and Toubal (2015), Kallel et al. (2018), Hamad et al. (2018*a*, *b*; 2021*a*, *b*), Elubid et al. (2019), Zeqiri et al. (2019), Nekkoub et al. (2020), Kerbati et al. (2020), Besser et al. (2021) and Brahmi et al. (2021) have highlighted water-related challenges in the study area and neighbouring regions, emphasizing issues of water availability, quality and sustainability.

Comprehensively assessing groundwater quality within the Tebessa aquifer system, a primary source for various needs, is essential. Challenges such as hydric stress, climatic aridity, rapid urbanization, and population growth have led to overexploitation and degradation of aquifer quality. This study focuses on factors contributing to groundwater quality decline to contribute to a deeper scientific understanding and develop sustainable solutions.

The Water Quality Index (WQI) method serves as a pivotal tool, offering a concise representation of overall water health by synthesizing diverse parameters. It enables policymakers, scientists, and resource managers to gauge water pollution extent, track trends, and allocate resources for remediation strategies, fostering a standardized framework for evaluating water quality.

Geographic Information Systems (GIS) technology, renowned for systematizing and analysing geographical data, emerges as a foundational instrument in hydrogeological modelling. Coupled with the WQI, GIS provides a dynamic framework for assimilating water quality parameters into comprehensive spatial analyses, aiding in effective resource management and policy formulation.

Research on water scarcity in the semi-arid region of North Africa, as evidenced by the works of Hamed et al. (2018, 2023), Bensoltane et al. (2021), Benmarce et al. (2021, 2023), and Ncibi et al. (2021, 2022), underscores the urgency and complexity of the addressing water scarcity issues. The study employs a multiparameter approach, including pH, Total Dissolved Solids (TDS), and crucial ions, synthesized and assimilated using GIS capabilities, resulting in meticulously constructed maps. These maps provide insights into spatial variations, culminating in a unified integrated map stratified into priority classes, representing a pragmatic depiction of groundwater quality across the studied region.

The overarching objective of this study is to comprehensively assess and enhance the understanding of groundwater quality in semiarid regions, particularly Tebessa. The primary aim is to evaluate groundwater quality, identify key influences, integrate spatial and analytical approaches, and formulate management strategies. The findings are expected to inform evidence-based policies and strategies to mitigate risks associated with water scarcity and preserve water resources critical for human well-being in environmentally sensitive areas.

2. Study Area

The geological context of North Africa forms an integral segment within the broader framework of African geology. This intricate geological setting holds paramount significance in unraveling the geological history and dynamics of the African continent (Rouabhia et al., 2004; Bagwan et al., 2023; Sankar et al., 2023; Orabi et al., 2023). In the border region between Algeria and Tunisia, all the collapse trenches intersect atlas structures of the Late Lutetian age. The extensional phase of the Miocene is evidenced by the formation of the Oulad Soukies, Foussana-Kasserine trenches, and the El Ma Labiod basin. The substrate of the Tebessa and Hammamet trenches is composed of a mosaic of horsts and grabens. Four successive stages have been identified during the development of the Tebessa trench: The

130

first stage occurred during the Lower Villafranchian (Upper Pliocene). The second stage occurred during the Upper Villafranchian. The third stage occurred at the end of the Middle Pleistocene. And the fourth stage occurred at the end of the Upper Pleistocene. The subsidence process is still ongoing, as evidenced by three seismic events in 1995. This is parallel to the uplifting of the graben margins, where the subsurface sank in the central part during the final collapse stage. This ongoing geodynamic activity sheds light on the complex tectonic evolution of the region.

The Tebessa-Morsott plain (35°24' to 35°35' N latitude and 7°50' to 8°10' E longitude) is situated in the northeastern region of Algeria at 28 km from the international border, and 230 km from the Mediterranean Sea. Spanning an area of 974.4 km², this basin stands as a host to significant aquifers that play a crucial role in the region (Figure 1). The region is marked by a semi-arid climate featuring hot and arid summers, contrasting with cold winters. The annual precipitation ranges from 200 mm to 350 mm, indicative of the region's arid nature. The summer temperatures can surge to 45°C.

The Tebessa-Morsott plain belongs to the Merdja subwatershed and is drained by the Oued Ksob stream. It boasts an elongated North-West to South-East orientation and encompasses a vast depression hemmed in by mountainous terrain. The altitudinal variation spans from 1712 meters to 700 meters, adhering to the geological structure of the North Auresian (Aures Nememcha) region within the Saharan Atlas.

Numerous researchers have diligently explored the geological context of the study region, as evidenced by the works of Mouici et al. (2017), Tamani et al. (2019), Boulemia et al. (2021), Zerzour et al. (2020; 2021), Taib et al. (2022; 2023), Mahleb et al. (2022), Chibani et al. (2022), Benyoucef et al. (2023) and Zighmi et al. (2023). The region is characterized by the Triassic diapirs of Jebel Jebissa, constituting the oldest geological outcrop in the Tebessa region. These formations consist of sandstone clay passing to gypsum limestone. A substantial Plio-Quaternary infill within the Tebessa Collapse Ditch substantiates the existence of a considerable groundwater reservoir in the region.

It consists of sand, alluviums, and limestone pebbles. The Maastrichtian carbonate formations outcrop in the South-West and North-East edge of the basin, whereas the Turonian limestone appears in the East (Figure 2). These serve as important karstic reservoirs of the region. Because of their significant depth in the center of the basin, the potential of these reservoirs remains untapped within the plain.

3. Materials and Methods

3.1. Field and Laboratory Investigations

In February 2019, a comprehensive groundwater sampling campaign was executed across three distinct locations: Merdja, Bekkaria and Hammamet. This operation aimed to assess the hydrochemical characteristics of the sampled groundwater. The collected groundwater samples underwent an analysis to ascertain their chemical composition and properties.

Analytical scrutiny was conducted in the laboratory setting, employing standardized methodologies outlined by the American Public Health Association (APHA) in the year 1995. The range of eight key parameters was meticulously investigated in each groundwater sample. Calcium (Ca^{+2}), Mg^{+2}, bicarbonate (HCO_3^-), chloride (Cl^-), sulfate (SO_4^{-2}), potassium (K^+), sodium (Na^+), and major cations (Ca^{+2}, Mg^{+2}, Na^+, and K^+) formed the focal points of the investigation. The determination of major cations (namely calcium, sodium, magnesium and potassium) was achieved via the utilization of the ICP-Mass spectrometer method. The quantification of bicarbonate (HCO_3) content involved a volumetric titration process employing hydrochloric acid (HCl) as the reagent. For the assessment of sulfate, a spectrophotometric turbidimetry method was employed, while chloride (Cl^-) content was quantified using a volumetric titration procedure involving silver nitrate ($AgNO_3$) and potassium dichromate ($K_2Cr_2O_7$). Moreover, bicarbonate (HCO_3) and carbonate (CO_3) concentrations were evaluated through Portamess analysis using titration with hydrochloric acid (HCl), alongside the utilization of phenolphthalein and methyl orange as indicator reagents (Selvam et al. 2013). This method yielded a dataset that improves our kind of the hydrochemical composition of the sampled groundwater across these locations.
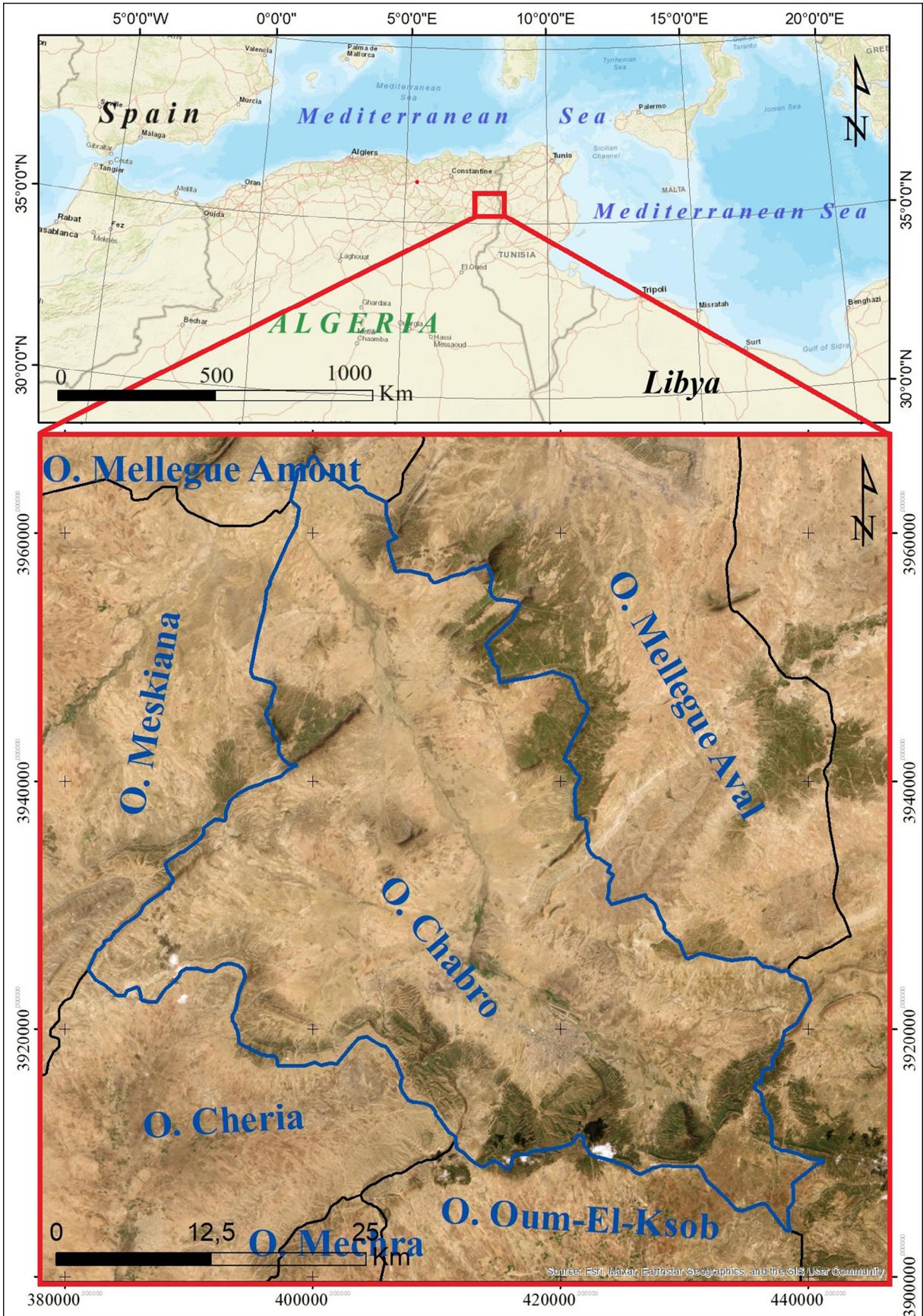
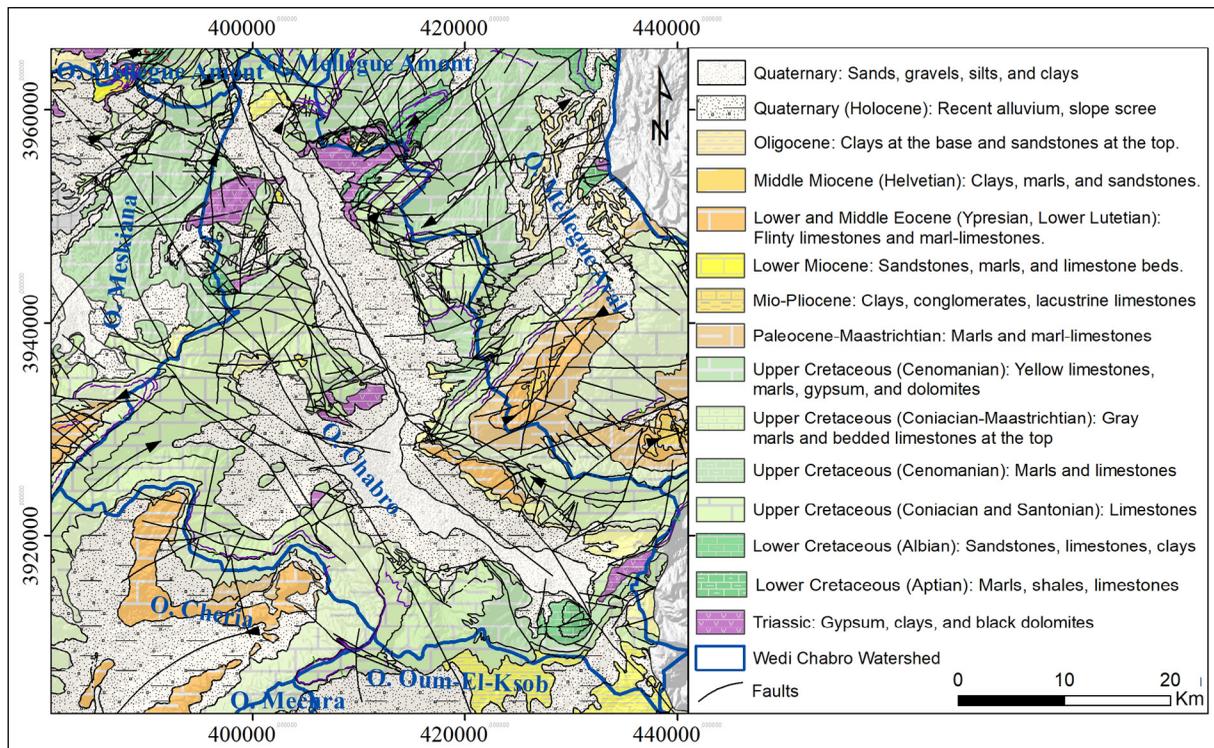Figure 1- Geographic location of the study area.

Figure 2- Simplified geological map of study area.

3.2. Geospatial Data Collection, Integration, and Interpolation

The accurate determination of sampling points, encompassing their precise latitude, longitude, and elevation coordinates, was achieved through the utilization of the GARMIN 12-Channel GPS device in the fieldwork. These geographical coordinates, once established, were combined with the groundwater parameters following preparation within the Excel-pro Program. This dataset was subsequently imported into a GIS platform, serving as the foundation for further analytical and digitization processes. The dataset, now in the form of point data, was integrated into the ArcGIS 10.8 software, where it constituted a distinct point layer. To facilitate advanced analyses and visualization, a geo-database was established. This facilitated the generation of spatial distribution maps that depicted the prevalence of selected water quality parameters across the studied region (Bairu et al., 2013). Spatial interpolation, a technique pivotal in environmental sciences, involves predicting values at unknown points based on known values at neighbouring points. Among the plethora of interpolation methods, two widely employed ones

are Inverse Distance Weighting (IDW) and Ordinary Kriging (OrK). Both methods fundamentally rely on the concept of spatial autocorrelation, wherein samples that are spatially proximate tend to exhibit similar characteristics.

The implementation of IDW and OK necessitates the determination of observation quantities for predictions. In this context, the search window's scope should encompass these observations, thus encapsulating an area surrounding the point of prediction. The configuration of this search window is determined based on empirical knowledge pertaining to the phenomenon being investigated (Zarco-Perello and Simões, 2017). IDW method estimates data values for unknown locations by averaging the available values from sampled data points (Setianto and Triandini, 2013).

3.3. Calculation of WQI

To assess the water quality of the basin, the WQI is a valuable tool that summarizes multiple water parameters into a concise numerical representation. This index method is particularly aligned with the

guidelines for drinking water quality established by the World Health Organization (WHO). By converting an array of complex variables into a singular one- or two-digit number, the WQI simplifies the interpretation of extensive monitoring data. Water quality indices offer a streamlined means of monitoring and managing water quality. They serve as a convenient instrument for assessing trends in regional water quality and aiding decision-makers in evaluating the efficacy of specific interventions aimed at improving water quality (Li et al., 2019). The computation of the WQI involves four sequential steps. In the initial step, each of the nine water quality parameters is assigned a weight (W_i) based on its relative significance in determining the overall quality of water for drinking purposes. Notably, the assignment of weights was informed by their individual importance, parameters such as chloride, sulfate, and sodium were assigned a weight of 3, while calcium, magnesium, bicarbonate, and potassium were assigned a weight of 2 (Table 1).

The subsequent step involves the calculation of the relative weight (W_i) according to the Equation 1:

$$w_i = \frac{w_i}{\sum_{i=1} w_i} \qquad (1)$$

Where "Wi" represents the relative weight, "wi" is the weight of each parameter, and "n" is the number of parameters.

Following this, a quality rating scale (qi) is assigned to each parameter (Equation 2). This scale is derived by dividing the concentration (Ci) of each chemical parameter in a water sample by its standard (Si) as outlined by WHO guidelines.

$$q_i = (C_i / S_i) \times 100 \qquad (2)$$

Equation (2) captures this rating, with qi signifying the quality rating, Ci representing the concentration of each chemical parameter in milligrams per liter (mg/l), and Si denoting the WHO drinking water standard for each parameter according to WHO guidelines. The Sub-Index (SI) for each parameter (i) is subsequently computed using the (Equation 3):

$$SI_i = W_i \, q_i \qquad (3)$$

The overall WQI is obtained by summing the individual SIi values (Equation 4):

$$WQI = \Sigma \, SI_i \qquad (4)$$

The calculated WQI values are generally categorized into five distinct classes: Excellent, good, poor, very poor, and unfit for drinking purposes (Table 2). This classification aids in communicating the quality of groundwater samples, thus supporting informed decision-making (Tiwari et al., 2014).

Table 2- Classification of WOI range and category of water.

WQI Range	Category of water
<50	Excellent water
50-100	Good water
100-200	Poor water
200-300	Very Poor water
>300	Unfit for drinking purpose

4. Discussions

The assessment of groundwater quality holds significant importance in environmental evaluation.

Table 1- Relative weight of chemical parameters.

Chemical parameters	WHO Standard	Weight(wi)	Relative weight(Wi)
Na^+	200	3	0.17
Ca^{2+}	75	2	0.12
K^+	12	2	0.12
Cl^-	250	3	0.17
SO_4^{-2}	250	3	0.17
HCO_3^-	120	2	0.12
Mg^{2+}	50	2	0.12
Total		$\Sigma wi = 17$	$\Sigma Wi = 0.99$

Key statistics for 16 groundwater samples have been compiled through chemical analyses, as outlined in Table 3. Furthermore, the correlation matrix analysis, presented in Table 4, provides insights into the complex relationships among various groundwater quality parameters.

The analysis gives a comprehensive snapshot of key statistical parameters for water quality in groundwater samples, shedding light on the range, central tendency, and variability of various constituents. The maximum and minimum values highlight the broad spectrum of concentrations, indicating substantial variability in the groundwater composition. Mean values provide an average measure for each parameter, showcasing the typical concentration levels. Standard deviations quantify the dispersion around the mean, elucidating the consistency or variability in the dataset. Medians offer a central value, indicating the middle point in the ordered dataset and providing a robust measure of central tendency. Table 4, the correlation matrix, unveils the intricate relationships between groundwater quality parameters. Notably, the correlation coefficients signify the degree and direction of associations between different ions. The strong positive correlation between Ca^{+2} and Cl^- suggests a potential common

source or geochemical processes linking these ions. Additionally, the correlations help identify potential influences or interactions, providing valuable insights for groundwater management and environmental assessment. These results contribute to a nuanced understanding of groundwater characteristics, aiding in the formulation of strategies for resource preservation and contamination prevention in the studied area.

In the study area the ions examined, namely HCO^{-3}, SO_4^{-2}, Cl^-, Ca^{+2}, Mg^{+2}, K^+, and Na^+, a noteworthy observation is the relatively low variability exhibited by their concentrations. Specifically, the bicarbonate content fluctuates between 173.24 and 341.16 mg/l, sulfate ranges from 57.60 to 500 mg/l, calcium ranges from 45.62 to 161 mg/l, potassium varying from 2.70 to 7.5 mg/l, sodium spanning 12.50 to 23.10 mg/l and magnesium varying between 17.01 and 61 mg/l. Of particular significance is the elevated concentration of chloride, demonstrating a wide variability from 37.99 to 291.3 mg/l. Examining the interrelationships between parameters. The chloride content is strongly correlated with magnesium (R= 0.62) and calcium (R = 0.61) These correlations can indeed indicate an increase in groundwater salinity underscore augmented groundwater salinity, such

Table 3-Normal statistics of water quality parameters of groundwater samples.

STATISTICS	K(mg/l)	Mg(mg/l)	Ca(mg/l)	Na(mg/l)	Cl(mg/l)	SO$_4$(mg/l)	HCO$_3$Meq/l
Maximum	7.5	61	161	23.10	291.3	500	341.16
Minimum	2.70	17.01	45.62	12.50	37.99	57.60	173.24
Average	5.23	37.31	94.27	17.88	147.06	294.70	261.94
Standarddeviation	1.47	14.29	28.70	3.03	76.89	125.15	55.24
Median	4.90	35.49	84.16	17.88	141.80	290	261.94

Table 4- Correlation matrix analysis result of the groundwater quality parameters.

Parameters	Mg^{+2}	K$^+$	Ca^{+2}	Na$^+$	SO$_4^{-2}$	HCO$_3^-$	Cl$^-$
Mg^{+2}	1						
K$^+$	-0.25	1					
Ca^{+2}	0.61	-0.36	1				
Na$^+$	-0.02	0.44	0.12	1			
SO$_4^{-2}$	-0.20	0.28	-0.13	0.05	1		
HCO$_3^-$	0.37	-0.48	0.28	-0.31	0.09	1	
CL$^-$	0.62	-0.21	0.59	-0.07	-0.46	0.02	1

findings provide valuable insights into the complex hydrochemical interactions at play within the Merdja aquifer region. By juxtaposing statistical analyses, correlation evaluations, and parameter concentrations, this study offers a comprehensive understanding of the groundwater quality dynamics within the investigated area. These insights contribute not only to the scientific understanding of the aquifer's hydrochemistry but also to the broader objectives of water resource management and environmental protection.

4.1. Spatial Variability Physicochemical Parameter

Calcium: Groundwater contains calcium due to the dissolution of carbonate formations surrounding the aquifer and it is also influenced by the presence of gypsum marl, dolomite minerals and evaporative deposits. The MCL for Ca^{+2} in drinking water is 75 mg/l. Observed Ca^{+2} concentrations range from 45.62 to 161 mg/l. The spatial distribution map portraying calcium concentrations has been formulated and is illustrated in Figure 3.

Sodium: It appears that sodium ions come from the leaching of Triassic gypsum formations near Djebissa. The gypsiferous marl forming the rock substrate of the aquifer generates these ions through ion exchange and evaporation processes. The MCL for Na+ in drinking water is set at 200 mg/l. The measured Na+ concentrations range from 12.5 to 23.10mg/l. A spatial map depicting the spatial variability of sodium concentrations is presented in Figure 3.

Potassium: The presence of potassium in groundwater is attributed to the use of fertilizers in nearby agricultural lands The MCL for K^+ in drinking water is defined as 12 mg/l. The observed K^+ concentrations range from 2.7 to 7.50 mg/l. A spatial map illustrating potassium concentration variations has been formulated and is exhibited in Figure 3.

Magnesium: The presence of magnesium due to the dissolution of dolomite limestones formations. The MCL for SO_4^{-2} in drinking water is set at 50 mg/l. The observed SO_4^{-2} concentrations span from 17.01 to 61 mg/l. A spatial map depicting the distribution of sulphate concentrations has been constructed and is presented in Figure 3.

Sulphate: the presence of sulphate it attributed to the dissolution of gypsum within gypsiferous marls and the leaching of evaporites and atmospheric deposition, industrial discharges. The MCL for SO_4^{-2} in drinking water is set at 250 mg/l. The observed SO_4^{-2} concentrations span from 57.6 to 500 mg/l. A spatial map depicting the distribution of sulphate concentrations has been constructed and is presented in Figure 3.

Chloride: Chloride content arises from the leaching of evaporites as well as sand, clay and gypsum deposits covering a significant basin area. Additionally, industrial activities contribute to chloride concentration. The MCL for Cl- in drinking water is established at 250 mg/l. The observed Cl- concentrations range from 37.99 to 291.30 mg/l. A spatial map portraying the spatial distribution of chloride concentrations has been formulated and is displayed in Figure 3.

Bicarbonate: Bicarbonate is present due to the dissolution of carbonate formations that surround the aquifer. The MCL for HCO_3^- in drinking water is specified as 120 mg/l. Observed HCO_3^- concentrations span from 173.24 to 341.16 mg/l. A spatial map outlining the spatial distribution of bicarbonate concentrations has been developed in Figure 3.

4.2. Mapping Groundwater Quality Index

The generation of the groundwater quality map (Figure 4) entailed is based on the classification process framework outlined in Table 5, and executed using ArcGIS software.

The intricate spatial distribution of groundwater quality is a product of various interacting factors, including lithological characteristics, hydrodynamic behaviour of groundwater, prevailing climatic conditions, influx of wastewater, and potential sources of pollution.

Integral to this endeavour is the creation of a WQI map, a visual representation that encapsulates a comprehensive synthesis of water quality parameters. This is due to the Kriging geostatistical technique renowned for its ability to yield spatial interpolations of complex datasets. The WQI values were judiciously
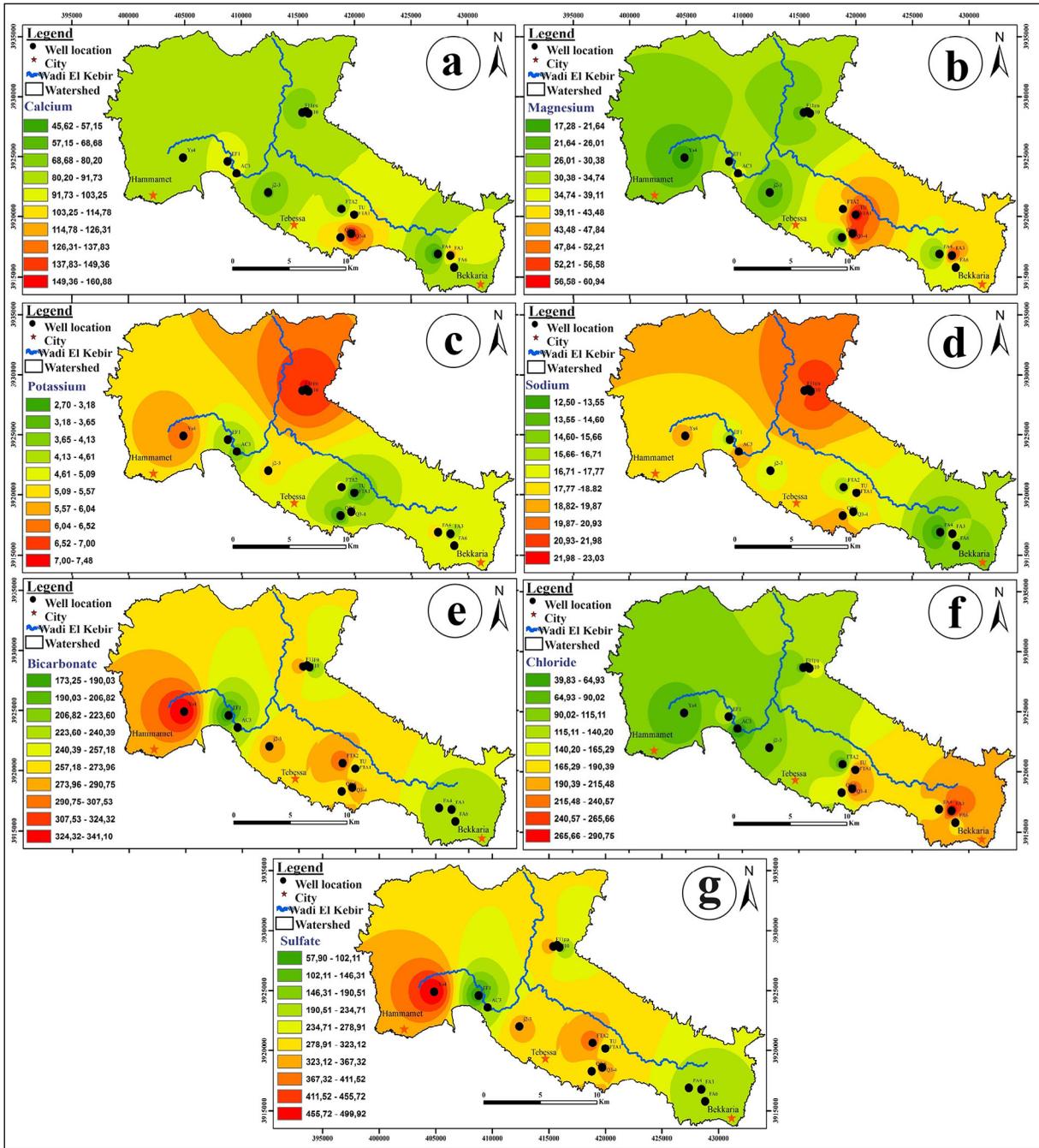
Figure 3- Spatial distribution of physiochemical parameters: a) Calcium (Ca^{+2}); b) Magnesium (Mg^{+2}); c) Potassium (K^+); d) Sodium (Na^+); e) Bicarbonate (HCO_3^-); f) Chlorite (Cl^-); g) Sulfate (SO_4^{-2}).

classified into four distinct ranges, namely excellent water (<50), good water (50-100), poor water (100-200), and very poor water (200-300).

The classification of the water in the study area is good except for well Q3-4 which is characterized by poor quality.

This insightful geospatial analysis accentuates the intricate interplay of myriad factors influencing groundwater quality distribution. Such revelations hold far-reaching implications, particularly in the realms of resource management and environmental safeguarding. The synergy of water quality indices, advanced geostatistical methodologies, and GIS tools
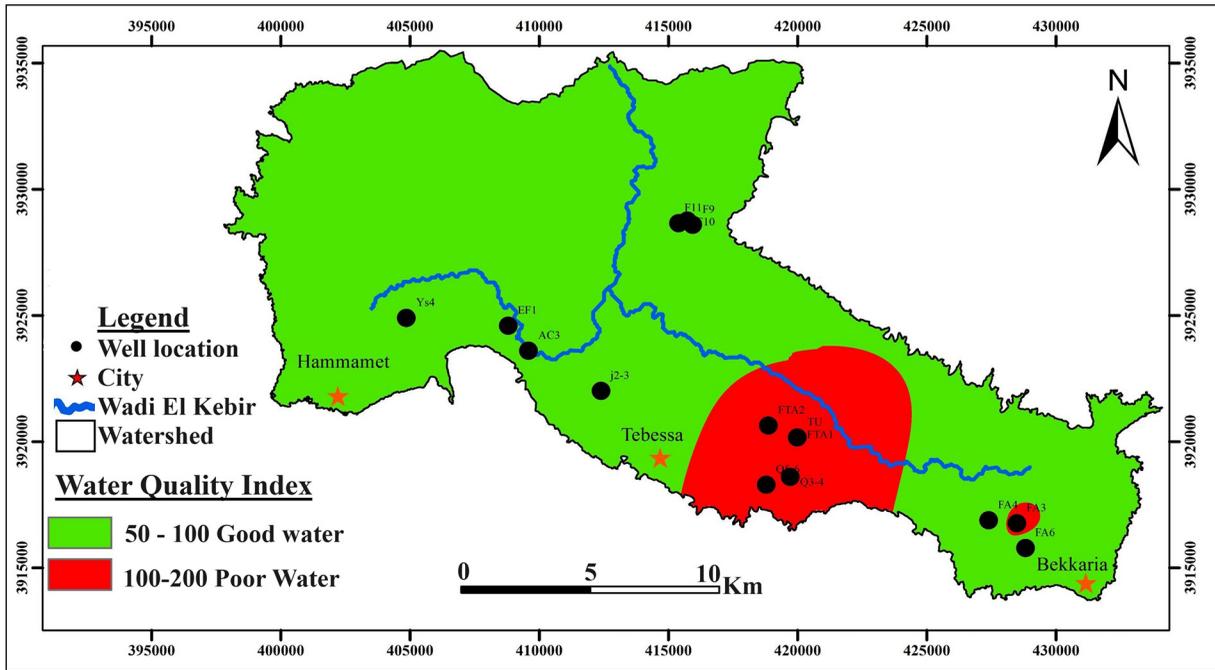
Figure 4- Spatial distribution map of water quality index in Merdja plain.

Table 5- Qi, SI$_i$, WQI and water classification of each groundwater samples of study area.

Sample	Na$^+$		Ca^{+2}		K$^+$		Mg^{+2}		Cl$^-$		SO$_4^{-2}$		HCO$_3^-$		WQI	Class
	Qi	SLi	Qi	SLi	Qi	SLi	Qi	SLi	Qi	SLi	Qi	SLi	Qi	SLi		
EF1	8.05	1.37	133.60	16.03	35.83	4.30	62.22	7.47	56.72	9.64	23.04	3.92	162.67	19.52	62.25	Good
j2-3	8.50	1.45	89.33	10.72	43.33	5.20	44.22	5.31	44.52	7.57	139.20	23.66	181.98	21.838	75.74	Good
AC3	10.00	1.70	122.83	14.74	32.50	3.90	72.90	8.75	18.12	3.08	84.48	14.36	223.67	26.84	73.37	Good
FA3	8.55	1.45	172.93	20.75	35.83	4.30	113.54	13.62	116.52	19.81	71.20	12.10	224.68	26.962	99.00	Good
FA4	6.25	1.06	60.83	7.30	44.17	5.30	46.24	5.55	66.40	11.29	90.80	15.44	204.35	24.522	70.46	Good
FA6	7.35	1.25	105.80	12.70	40.83	4.90	70.00	8.40	68.30	11.61	92.00	15.64	233.38	28.006	82.50	Good
FTA1	9.15	1.56	134.67	16.16	24.17	2.90	121.06	14.53	90.48	15.38	103.68	17.63	196.00	23.52	91.67	Good
FTA2	7.95	1.35	99.39	11.93	40.00	4.80	82.40	9.89	24.08	4.09	168.00	28.56	284.30	34.116	94.74	Good
T3	10.75	1.83	106.83	12.82	59.17	7.10	87.50	10.50	40.00	6.80	138.00	23.46	244.00	29.28	91.79	Good
TU	6.90	1.17	103.25	12.39	31.67	3.80	76.20	9.14	23.64	4.02	111.20	18.90	281.62	33.794	83.22	Good
Q3-4	8.35	1.42	214.67	25.76	40.83	4.90	122.00	14.64	102.00	17.34	138.40	23.53	264.17	31.7	119.29	Poor
Q5-6	9.90	1.68	149.33	17.92	22.50	2.70	36.00	4.32	55.20	9.38	116.00	19.72	274.17	32.9	88.63	Good
Ys4	9.45	1.61	112.21	13.47	52.50	6.30	40.08	4.81	28.36	4.82	200.00	34.00	144.37	17.324	82.33	Good
F10	11.55	1.96	100.47	12.06	62.50	7.50	70.98	8.52	59.96	10.19	120.00	20.40	172.83	20.74	81.37	Good
F9	10.95	1.86	114.36	13.72	55.00	6.60	67.10	8.05	73.99	12.58	27.95	4.75	170.83	20.5	68.07	Good
F11	9.45	1.61	101.53	12.18	57.50	6.90	34.02	4.08	15.20	2.58	180.00	30.60	163.43	19.612	77.57	Good
EF1	8.05	1.37	133.60	16.03	35.83	4.30	62.22	7.47	56.72	9.64	23.04	3.92	162.67	19.52	62.25	Good

culminate in a holistic understanding that guides strategic decision-making processes and contributes to the sustainable management of vital water resources.

5. Determination of chemical facies

5.1. Piper diagram

According to the ionic relationship between the hydrochemical parameters in the study area and their distribution by plotting the major cations and anions on the Piper trilinear diagram, it is observed that there are two dominant facies: Calcic sulphate and calcic chloride Due to the dissolution of carbonate formations and gypsum.

5.2. The origins of chemical elements

The calcium often originates from geological formations rich in minerals such carbonate and gypsum, these geological formations play a crucial role in the presence and availability of calcium in the environment the analysis of diagram shows that 5 out of 16 samples have a carbonate origin (Figures 5, 6, 7 and 8).

The presence of chloride and sodium is linked to the dissolution of triassic formations. The diagram indicates the existence of another source of sodium in the product when water interacts with clay minerals leading to the fixation of calcium ions after the release of tow sodium ions.

Salinity is associated with the dissolution of evaporate or carbonate formations and Base Exchange as suggested by the interpretation of previous diagram.

6. Results

The preservation of groundwater quality is pivotal for sustaining life in semiarid regions heavily reliant on this precious resource. This study underscores the intricate interplay of factors impacting groundwater quality within the Tebessa-Morsott plain of North-eastern Algeria. The aquifer's vulnerability to contamination, coupled with escalating demands, compels a comprehensive assessment to ensure its sustainability.
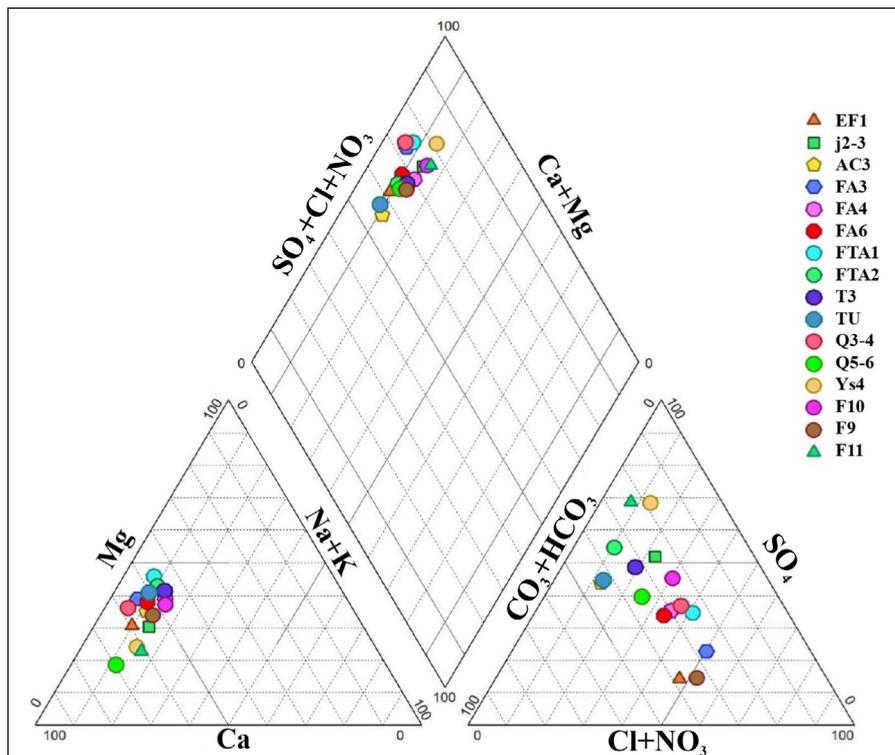

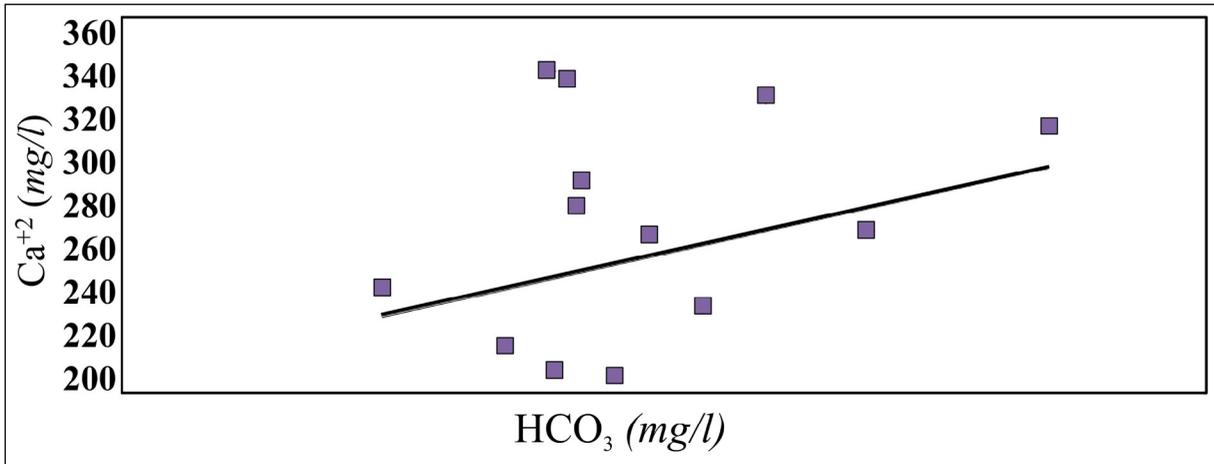Figure 5- Chemical facies of water using the Piper diagram.

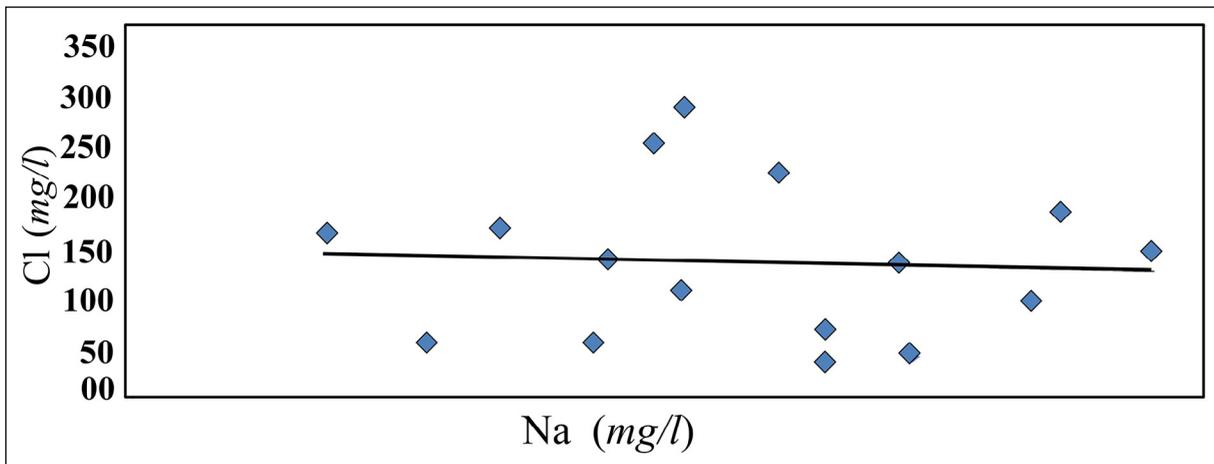Figure 6- Ca^{+2} vs HCO$_3^-$ in Merdja plain.
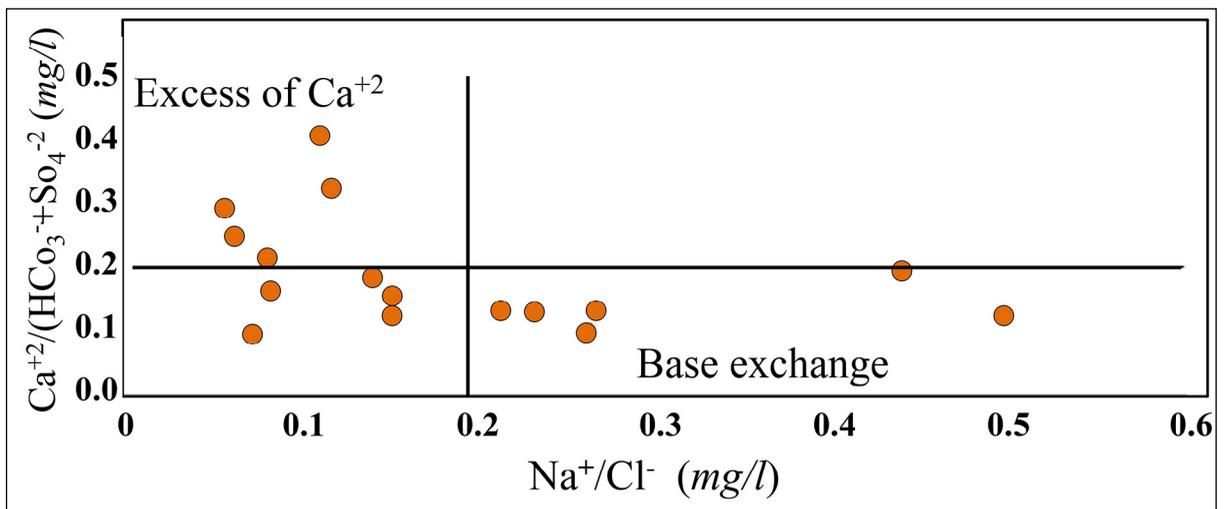

Figure 7- Cl$^-$ vs Na$^+$ in Merdja plain.

Figure 8- Base Exchange in the Merdja plain.

Groundwater quality is not only a product of natural processes but is also profoundly influenced by anthropogenic activities. Increased agricultural practices, accentuated by chemical pesticide use, contribute to the degradation of water quality. Complex interactions between the aquifer and surrounding soil, lithology, and climatic conditions further exacerbate the challenge. Understanding these dynamics is essential for crafting effective management strategies.

The WQI serves as a powerful tool for quantifying water quality. This method simplifies complex data into a single numerical value, allowing for easy interpretation and informed decision-making. Integrating GIS amplifies this approach, enabling spatial analyses that unveil trends and patterns, aiding resource management and policy formulation.

Results underscore the significance of calcium, sodium, potassium, sulphate, chloride, and bicarbonate concentrations in groundwater. Strong correlations reveal intricate relationships, shaping the hydrochemical landscape. By mapping these parameters, spatial nuances become apparent, guiding targeted interventions.

Crucially, the WQI map reflects the intricate web of influences on groundwater quality. Wells with excellent water quality (WQI <50) are identified, while those with poor and very poor quality signal intervention needs. This geospatial understanding supports resource allocation and decision-making processes.

The study's objective to enhance understanding aligns with sustainable management aspirations. Its findings inform policies, interventions, and strategies vital for navigating the challenges of water scarcity. By synergizing scientific rigor, geospatial analysis, and multidisciplinary insights, this study paves the way for safeguarding groundwater quality in semiarid regions, ensuring the continued availability of this invaluable resource for generations to come.

Addressing the multifaceted challenges of water scarcity and declining groundwater quality in semiarid regions necessitates a comprehensive approach. Integrated management strategies, involving collaboration between government agencies, local communities, and scientific institutions, should encompass regulatory measures to control pollution sources while promoting sustainable practices. A robust groundwater monitoring network is crucial for tracking water quality changes over time, fostering transparency and informed decision-making. Incorporating climate resilience strategies, education on sustainable water practices, economic incentives, and cross-border collaboration can enhance groundwater preservation efforts. Sustained research and innovation are vital to understanding complex interactions and developing effective solutions. Policy integration across sectors ensures holistic management, ensuring equitable and sustainable use of groundwater resources while considering environmental protection and land use. By embracing these recommendations, stakeholders can navigate the challenges posed by water scarcity and safeguard the availability of safe water for current and future generations.

Acknowledgments

References

Bagwan, W. A., Gavali, R. S., Maity, A. 2023. Quantifying soil organic carbon (SOC) density and stock in the Urmodi River watershed of Maharashtra, India: Implications for sustainable land management. Journal of Umm Al-Qura University for Applied Sciences, 1-17.

Bairu, A., Tadesse, N., Amare, S. 2013. Use of geographic information system and water quality index to assess suitability of groundwater quality for drinking purposes in Hewane areas, Tigray, Northern Ethiopia. Ethiopian Journal of Environmental Studies and Management, 6 (2), 110-123.

Benmarce, K., Hadji, R., Zahri, F., Khanchoul, K., Chouabi, A., Zighmi, K., Hamed, Y. 2021. Hydrochemical and geothermometry characterization for a geothermal system in semiarid dry climate: The case study of Hamma spring (Northeast Algeria). Journal of African Earth Sciences, 182, 104285.

Benmarce, K., Hadji, R., Hamed, Y., Zahri, F., Zighmi, K., Hamad, A., Gentilucci M., Ncibi, K., Besser, H. 2023. Hydrogeological and water quality analysis

of thermal springs in the Guelma region of North-Eastern Algeria: A study using hydrochemical, statistical, and isotopic approaches. Journal of African Earth Sciences, 205, 105011.

Bensoltane, M. A., Zeghadnia, L., Hadji, R. 2021. Physicochemical Characterization of Drinking Water Quality of the Communal Water Distribution Network in Souk Ahras City/Algeria. Civil Engineering Research Journal, 12 (02).

Benyoucef, A. A., Gadri, L., Hadji, R., Slimane, H., Mebrouk, F., Hamed, Y. 2023. Empirical graphical and numerical model for the schematization of underground mining operations in the heterogeneous rock masses, case of Boukhadra mine, Algeria. Arabian Journal of Geosciences 16 (3), 165.

Besser, H., Dhaouadi, L., Hadji, R., Hamed, Y., Jemmali, H. 2021. Ecologic and economic perspectives for sustainable irrigated agriculture under arid climate conditions: An analysis based on environmental indicators for southern Tunisia. Journal of African Earth Sciences, 104134.

Boulemia, S., Hadji, R., Hamimed, M. 2021. Depositional environment of phosphorites in a semiarid climate region, case of El Kouif area (Algerian–Tunisian border). Carbonates and Evaporites, 36 (3), 1-15.

Brahmi, S., Baali, F., Hadji, R., Brahmi, S., Hamad, A., Rahal, O., Zerrouki, H., Saadali B., Hamed, Y. 2021. Assessment of groundwater and soil pollution by leachate using electrical resistivity and induced polarization imaging survey, case of Tebessa municipal landfill, NE Algeria. Arabian Journal of Geosciences, 14 (4), 1-13.

Chibani, A., Hadji, R., Hamed, Y. 2022. A combined field and automatic approach for lithological discrimination in semi-arid regions, the case of geological maps of bir later region and its vicinity, Nementcha mounts, Algeria. Geomatics, Landmanagement and Landscape (4), 7–26.

Drias, T., Toubal, A. C. 2015. Cartographie de la vulnérabilité a la pollution de la nappe alluviale de Tebessa-Morsott (bassin versant de l'Oued Ksob) extrême est algérien. LARHYSS Journal P-ISSN 1112-3680/E-ISSN 2521-9782, (22), 35-48.

Elubid, B., Huang, T., H. Ahmed, E., Zhao, J., M. Elhag, K., Abbass, W., Babiker, M. 2019. Geospatial distributions of groundwater quality in Gedaref state using geographic information system (GIS) and drinking water quality index (DWQI). International journal of environmental research and public health, 16 (5), 731.

Hamad, A., Baali, F., Hadji, R., Zerrouki, H., Besser, H., Mokadem, N., Legrioui R., Hamed, Y. 2018a. Hydrogeochemical characterization of water mineralization in Tebessa-Kasserine karst system (Tuniso-Algerian Transboundry basin). Euro-Mediterranean Journal for Environmental Integration, 3 (1), 7.

Hamad, A., Hadji, R., Bâali, F., Houda, B., Redhaounia, B., Zighmi, K., Legrioui, R., Brahmi S., Hamed, Y. 2018b. Conceptual model for karstic aquifers by combined analysis of GIS, chemical, thermal, and isotopic tools in Tuniso-Algerian transboundary basin. Arabian Journal of Geosciences, 11 (15), 409.

Hamad, A., Abdeslam, I., Fehdi, C., Badreddine, S., Mokadem, N., Legrioui, R., Hadji R. Hamed, Y. 2021a. Vulnerability characterization for multi-carbonate aquifer systems in semiarid climate, case of Algerian–Tunisian transboundary basin. International Journal of Energy and Water Resources, 1-14.

Hamad, A., Hadji, R., Boubaya, D., Brahmi, S., Baali, F., Legrioui, R., Abdeslam, I., Hidouri, B., Hamed, Y. 2021b. Integrating gravity data for structural investigation of the Youkous-Tebessa and Foussana-Talah transboundary basins (North Africa). Euro-Mediterranean Journal for Environmental Integration, 6 (2), 1-11.

Hamed, Y., Hadji, R., Redhaounia, B., Zighmi, K., Bâali, F., El Gayar, A. 2018. Climate impact on surface and groundwater in North Africa: A global synthesis of findings and recommendations. Euro-Mediterranean Journal for Environmental Integration, 3 (1), 25.

Hamed, Y., Hadji, R., Ahmadi, R., Ayadi, Y., Shuhab, K., Pulido-Bosch, A. 2023. Hydrogeological investigation of karst aquifers using an integrated geomorphological, geochemical, GIS, and remote sensing techniques (Southern Mediterranean Basin-Tunisia). Environment, Development and Sustainability, 1-33.

Kallel, A., Ksibi, M., Dhia, H. B., Khélifi, N. (Eds.). 2018. Recent advances in environmental science from the Euro-Mediterranean and surrounding regions: proceedings of Euro-Mediterranean Conference for Environmental Integration (EMCEI-1), Tunisia 2017. Springer International Publishing.

Kerbati, N. R., Gadri, L., Hadji, R., Hamad, A., Boukelloul, M. L. 2020. Graphical and Numerical Methods for Stability Analysis in Surrounding Rock of Underground Excavations, Example of Boukhadra Iron Mine NE Algeria. Geotechnical and Geological Engineering, 1-9.

Li, H., Smith, C. D., Wang, L., Li, Z., Xiong, C., Zhang, R. 2019. Combining spatial analysis and a drinking water quality index to evaluate monitoring data. International journal of environmental research and public health, 16 (3), 357.

Mahleb, A., Hadji, R., Zahri, F., Chibani, A., Hamed, Y. 2022. Water-Borne Erosion Estimation Using the Revised Universal Soil Loss Equation (RUSLE) Model Over a Semiarid Watershed: Case Study of Meskiana Catchment, Algerian-Tunisian Border. Geotechnical and Geological Engineering, 1-14.

Mouici R, Baali F, Hadji R, Boubaya D, Audra, P., Fehdi, C., Cailhol, D., Jaillet, S., Arfib, B. 2017. Geophysical, Geotechnical, and Speleologic assessment for karst-sinkhole collapse genesis in Cheria plateau (Algeria). Mining Science, 24, 59-71.

Ncibi, K., Hadji, R., Hajji, S., Besser, H., Hajlaoui, H., Hamad, A., Mokadem, N., Ben Saad, A., Hamdi, M., Hamed, Y. 2021. Spatial variation of groundwater vulnerability to nitrate pollution under excessive fertilization using index overlay method in central Tunisia (Sidi Bouzid basin). Irrigation and Drainage.

Ncibi, K., Mastrocicco, M., Colombani, N., Busico, G., Hadji, R., Hamed, Y., Shuhab, K. 2022. Differentiating Nitrate Origins and Fate in a Semi-Arid Basin (Tunisia) via Geostatistical Analyses and Groundwater Modelling. Water, 14 (24), 4124.

Nekkoub, A., Baali, F., Hadji, R., Hamed, Y. 2020. The EPIK multi-attribute method for intrinsic vulnerability assessment of karstic aquifer under semi-arid climatic conditions, case of Cheria Plateau, NE Algeria. Arabian Journal of Geosciences, 13 (15), 1-15.

Orabi, O. H., El-Sabbagh, A., Mansour, A. S., Ismail, H., Taha, S. 2023. Foraminifera study for the characterization of the Campanian/Maastrichtian boundary in Gebel Owaina, Nile Valley. Journal of Umm Al-Qura University for Applied Sciences, 1-19.

Rouabhia, A., Baali, F., Kherici, N., Djabri, L. 2004. Vulnérabilité et risque de pollution des eaux souterraines de la nappe des sables miocènes de la plaine d'El Ma El Abiod (Algérie). Science et changements planétaires/Sécheresse, 15 (4), 347-352.

Sankar, T. K., Ambade, B., Mahato, D. K., Kumar, A., Jangde, R. 2023. Anthropogenic fine aerosol and black carbon distribution over urban environment. Journal of Umm Al-Qura University for Applied Sciences, 1-10.

Selvam, S. I. J. D., Mala, R. I. J. D., Muthukakshmi, V. 2013. A hydrochemical analysis and evaluation of groundwater quality index in Thoothukudi district, Tamilnadu, South India. International Journal of Advanced Engineering Applications, 2 (3), 25-37.

Setianto, A., Triandini, T. 2013. Comparison of kriging and inverse distance weighted (IDW) interpolation methods in lineament extraction and analysis. Journal of Applied Geology, 5 (1).

Taib, H., Ben Abbas, Ch., Khiari, A., Hadji, R. 2022. Geomatics-based assessment of the Neotectonic landscape evolution along the Tebessa-Morsott-Youkous collapsed basin, Algeria, eomatics, Landmanagement and Landscape (3), 131–146.

Taib, H., Hadji, R., Hamed, Y., Bensalem, M. S., Amamria, S. 2023. Exploring neotectonic activity in a semiarid basin: A case study of the Ain Zerga watershed. Journal of Umm Al-Qura University for Applied Sciences, 1-14.

Tamani, F., Hadji, R., Hamad, A., Hamed, Y. 2019. Integrating Remotely Sensed and GIS Data for the Detailed Geological Mapping in Semi-Arid Regions: Case of Youks les Bains Area, Tebessa Province, NE Algeria. Geotechnical and Geological Engineering, 1-11.

Tiwari, A. K., Singh, P. K., Mahato, M. K. 2014. GIS-based evaluation of water quality index of ground water resources in West Bokaro Coalfield, India. Current world environment, 9 (3), 843.

Zarco-Perello, S., Simões, N. 2017. Ordinary kriging vs inverse distance weighting: Spatial interpolation of the sessile community of Madagascar reef, Gulf of Mexico. Peer J, 5, e4078.

Zeqiri, R. R., Riheb, H., Karim, Z., Younes, G., Mania, B., Aniss, M. 2019. Analysis of safety factor of security plates in the mine" Trepça" Stantërg. Mining Science, 26, 21.

Zerzour, O., Gadri, L., Hadji, R., Mebrouk, F., Hamed, Y. 2020. Semi-variograms and kriging techniques in iron ore reserve categorization: Application at Jebel Wenza deposit. Arabian Journal of Geosciences, 13 (16), 1-10.

Zerzour, O., Gadri, L., Hadji, R., Mebrouk, F., Hamed, Y. 2021. Geostatistics-Based Method for Irregular Mineral Resource Estimation, in Ouenza Iron Mine, Northeastern Algeria. Geotechnical and Geological Engineering, 1-10.

Zighmi, K., Zahri, F., Hadji, R., Benmarce, K., Hamed, Y. 2023. Polymetallic mineralization hosted in the Neogene sedimentary strata of the Algerian Tellian Range: A comprehensive overview. Mining of Mineral Deposits, 17 (2), 20-27.